

**Legends to Supplemental Figures.**

## Supplemental Figure S1

**Simulation of the effect of baseline subtraction errors.**

The observed raw fluorescence values (panel **A**, black circles) of cycle 1 to 15 were each used as baseline estimates resulting in 15 simulated PCR amplification curves. The baseline error in these simulated estimates ranged from -29% to +31%. Among the resulting curves, curve 8 (open circles) is closest to the curve resulting from an optimal baseline correction (see text). The results of this curve are shown as black circles in the other panels. The error in the baseline that was applied to each of these curves is used as X-axis label in panels **B** thru **E**. The 'baseline-corrected' data were analyzed with LinRegPCR (Ramakers et al. 2003) and the fit of the regression line in the window-of-linearity ( $R^2$ ; panel **B**), and the PCR efficiencies were estimated (panel **C**). Additionally the  $C_t$  value for each of the 'corrected' curves was determined (panel **D**). Estimates of the starting concentration were calculated with Eq. 2 (Box 1) using individual PCR efficiencies and individual  $C_t$  values ( $N_0$ ; panel **E**, open circles). Note that the fit of the regression lines to all but the most over-corrected curves is above  $R^2 = 0.996$  (panel **B**) but that the efficiency values derived from the slopes of these curves vary from 1.5 to 1.9 (panel **C**). In contrast, the  $C_t$  values vary only 0.3 cycles (panel **D** and **F**). The 100 times range in estimated starting concentrations (panel **E**, open circles) results from the variation in PCR efficiency extrapolated over  $C_t$  cycles. However, the mean of these obviously wrong PCR efficiencies, when used in Eq. 2, results in an almost constant starting concentration estimate (panel **E**, grey circles) that is also similar to the starting concentration resulting from the curve with the least error in baseline correction (panel **E**, black circle). Panel **F** shows an enlargement of panel **A** (from 15 to 23 cycles, fluorescence values of 1 to 10) and demonstrates that, for the range of applied baseline values, the  $C_t$  value deviates only about 0.3 cycles.

## Supplemental Figure S2.

**Developing chicken heart dataset**

Tissue samples of different parts of the developing chicken heart were amplified with primers for NppB and NDUF3. These samples were measured in three runs on the Roche LightCycler480.

**A.** PCR amplification curves showing the raw data, the data corrected with a baseline trend based on the cycles 3 thru 5, 3 thru 10, and 3 thru 15, and the data corrected with the LinRegPCR program described in this paper. Samples corrected with a baseline trend show the convex and concave curves that are characteristic of over- and under-estimation of the fluorescence baseline. Panels 2A1, 2A2, and 2A3 are the 3 independent PCR runs with the same samples.

**B.** Variation in PCR efficiency values derived after different baseline correction methods. PCR efficiencies were determined after application of a window-of-linearity per amplicon and per baseline correction method. The PCR efficiency variance is lowest in LinRegPCR-derived efficiencies. The p-values resulting from F-tests between variances found for both amplicons in different plates and for pooled data are given in Additional Table 1.

**C.** Relation between the PCR efficiencies derived with different baseline correction methods (left) and scatter plots of PCR efficiencies derived using a baseline trend against those derived with LinRegPCR (right). Results are separately given for NDUF3 (top) and NppB (bottom). No systematic relation between the different sets of PCR efficiencies could be observed. Correlation coefficients between LinRegPCR and BL 3-5, BL 3-10, or BL 3-15 were 0.210, 0.103, and 0.114, respectively, for NppB and 0.192, 0.085, and 0.002, respectively, for NDUF3.

**D.** Gene expression ratios in each part of the developing chicken heart were calculated with a PCR efficiency value per sample (top; according to Ramakers et al. 2003, but with a window-of-linearity per amplicon) and with the mean efficiency per amplicon per baseline correction method (bottom). Using the mean efficiency per amplicon reduces the variability. There is a high variability within and between the baseline-correction methods based on a baseline trend and conclusions about gene expression ratios in different parts of the heart would depend on the number of cycles that were included in the baseline trend. The results obtained with LinRegPCR in both panels reflect the known expression profile of NppB. ( Houweling et al. 2002)

**Legends to Supplemental Figures.**

## Supplemental Figure S3.

**Serial dilution data set**

A brain tissue sample was serially diluted (10 times/step; 4 steps) and for each dilution 5 replicate measurements were done with primers for EEF1A1. All measurements were done in 1 run on an ABI PCR system. The resulting dataset can be used to construct 3125 ( $=5^5$ ) different standard curves with one sample per dilution (Fig. 6).

**A.** PCR amplification curves showing the raw data, the data corrected with a baseline trend based on the cycles 3 thru 5, 3 thru 10, and 3 thru 15, and the data corrected with the LinRegPCR program described in this paper. Samples corrected with a baseline trend show the convex and concave curves that are characteristic of over- and under-estimation of the fluorescence baseline.

**B.** Variation in PCR efficiency values derived after different baseline correction methods. PCR efficiencies were determined after application of an individual window-of-linearity (left; according to Ramakers et al. 2003) or a common window-of-linearity (right). The PCR efficiency variance is lowest in LinRegPCR-derived efficiencies. The p-values resulting from F-tests between variances are given. Error bars indicate standard deviations.

**C.** Relation between the PCR efficiencies derived with different baseline correction methods (left) and scatter plots of PCR efficiencies derived using a baseline trend against those derived with LinRegPCR (right). No systematic relation between the different sets of PCR efficiencies could be observed. Correlation coefficients between LinRegPCR and BL 3-5, BL 3-10, or BL 3-15 were 0.027, 0.269, and 0.060, respectively.

**D.** Position of the fluorescence threshold and variation in the threshold cycle  $C_t$ . The fluorescence threshold ( $N_t$ ) for determining the  $C_t$  values was systematically moved between the upper and lower position indicated in the graph. For each of the 11 positions, the  $C_t$  value per sample was determined and the mean  $C_t$  per dilution (+/- the standard deviation) were calculated and plotted. The  $C_t$  variation is, as expected, largest at higher  $C_t$  values. Lowering of the fluorescence threshold leads to increasing within-dilution variation of the  $C_t$  values.

**E.** Observed starting concentrations for each of the input dilutions were calculated with the mean of the PCR efficiencies derived with each of the four baseline correction methods. Data points are shifted on the X-axis to avoid overlap. The results obtained with the baseline trend through cycles 3-10, and those of LinRegPCR closely fit to the  $Y=X$  expected for unbiased results. Baselines based on cycles 3-5 or 3-15 gave over- and underestimated results, respectively. The fact that the variation around the mean in the different result sets is similar reflects the fact that the  $C_t$  values hardly vary between baseline correction methods.

## Supplemental Figure S4.

**Huntington Disease data set**

Brain samples of 10 control persons (C) and 8 Huntington Disease (HD) patients were amplified with primers for ATG5 and PSMB5. This dataset served to study the effect of averaging efficiencies on the variation and the bias of the reported starting concentrations (Fig. 5).

**A.** PCR amplification curves showing the raw data, the data corrected with a baseline trend based on the cycles 3 thru 5, 3 thru 10, and 3 thru 15, and the data corrected with the LinRegPCR program described in this paper. Samples corrected with a baseline trend show the convex and concave curves that are characteristic of over- and under-estimation of the fluorescence baseline. PCR efficiencies are plotted for PSMB5 (panel 4A1) and ATG5 (panel 4A2)

**B.** Variation in PCR efficiency values derived after different baseline correction methods. PCR efficiencies were determined after application of a window-of-linearity per amplicon and per baseline correction method. The PCR efficiency variance is lowest in LinRegPCR-derived efficiencies. The p-values resulting from F-tests between variances are given. Error bars indicate standard deviations. There is no difference in PCR efficiency between control individuals and Huntington patients.

**C.** Relation between the PCR efficiencies derived with different baseline correction methods (left) and scatter plots of PCR efficiencies derived using a baseline trend against those derived with LinRegPCR (right). Results are separately given for PSMB5 (top) and ATG5 (bottom). No systematic relation between the different sets of PCR efficiencies could be observed. Correlation coefficients between LinRegPCR and BL 3-5, BL 3-10, or BL 3-15 were 0.022, 0.126, and 0.360, respectively, for PSMB5 and 0.034, 0.353, and 0.002, respectively, for ATG5.

**D.** Distribution of  $C_t$  values derived after application of the different baseline correction methods per amplicon in the control and Huntington disease group. The similar pattern in the different baseline correction methods reflects that the  $C_t$  value is hardly affected by the applied baseline.

**D.** PSMB5 / ATG5 gene expression ratio per patient, calculated with the PCR efficiency and  $C_t$  values derived after different baseline correction methods. The baseline subtraction methods based on a baseline trend show a slight increase in gene expression ratio. However, in none of the baseline subtraction methods there is a gene expression difference between the control and Huntington Disease group.

**References:**

Houweling, A.C., Somi, S., van den Hoff, M.J., Moorman, A.F.M. and Christoffels, V.M. (2002) Developmental pattern of ANF gene expression reveals a strict localization of cardiac chamber formation in chicken. *Anat Rec*, 266, 93-102.  
 Ramakers, C., Ruijter, J.M., Lekanne Deprez, R.H. and Moorman, A.F.M. (2003) Assumption-free analysis of quantitative real-time polymerase chain reaction (PCR) data. *Neurosci. Lett.*, 339, 62-66.

Supplemental Table 1. Descriptive statistics and F-test between variances of PCR efficiencies derived from datasets in which the baselines were set by the PCR system (linear baseline trend based on cycles 3-5, 3-10 or 3-15) and with the LinRegPCR program (Supplemental Fig. S2B). F-tests were performed to compare the efficiency variance per amplicon per plate and pooled over all plates.

N	plate		NppB			F (LRP/BL)	prob	NDUFB3			F (LRP/BL)	prob	
			Mean	stdev	Variance			Mean	stdev	Variance			
19	1	BL3_5	1.868	0.134	0.018	33.94	0.0000	1.919	0.241	0.058	102.7	0.0000	
		BL3_10	1.863	0.034	0.001	2.13	0.0586	1.863	0.068	0.005	8.08	0.0000	
		BL3_15	1.863	0.023	0.001	1.00	0.4970	1.875	0.031	0.001	1.74	0.1258	
		LinRegPCR	1.897	0.023	0.001			1.930	0.024	0.001			
20	2	BL3_5	1.758	0.042	0.002	2.53	0.0248	1.763	0.052	0.003	6.08	0.0001	
		BL3_10	1.905	0.067	0.005	6.37	0.0001	1.932	0.074	0.005	12.28	0.0000	
		BL3_15	1.898	0.044	0.002	2.71	0.0179	1.925	0.045	0.002	4.63	0.0008	
		LinRegPCR	1.900	0.027	0.001			1.929	0.021	0.000			
20	3	BL3_5	1.964	0.089	0.008	53.69	0.0000	1.818	0.036	0.001	3.40	0.0053	
		BL3_10	1.912	0.063	0.004	26.76	0.0000	2.049	0.085	0.007	18.91	0.0000	
		BL3_15	1.912	0.047	0.002	14.88	0.0000	1.978	0.062	0.004	10.07	0.0000	
		LinRegPCR	1.921	0.012	0.000			1.937	0.020	0.000			
			NppB						NDUFB3				
			Mean	stdev	Variance				Mean	stdev	Variance		
59	overall	BL3_5	1.863	0.127	0.016	28.39	0.0000	1.832	0.153	0.024	51.27	0.0000	
		BL3_10	1.894	0.060	0.004	6.37	0.0000	1.949	0.107	0.012	25.17	0.0000	
		BL3_15	1.891	0.044	0.002	3.44	0.0000	1.927	0.063	0.004	8.78	0.0000	
		LinRegPCR	1.906	0.024	0.001			1.932	0.021	0.000			

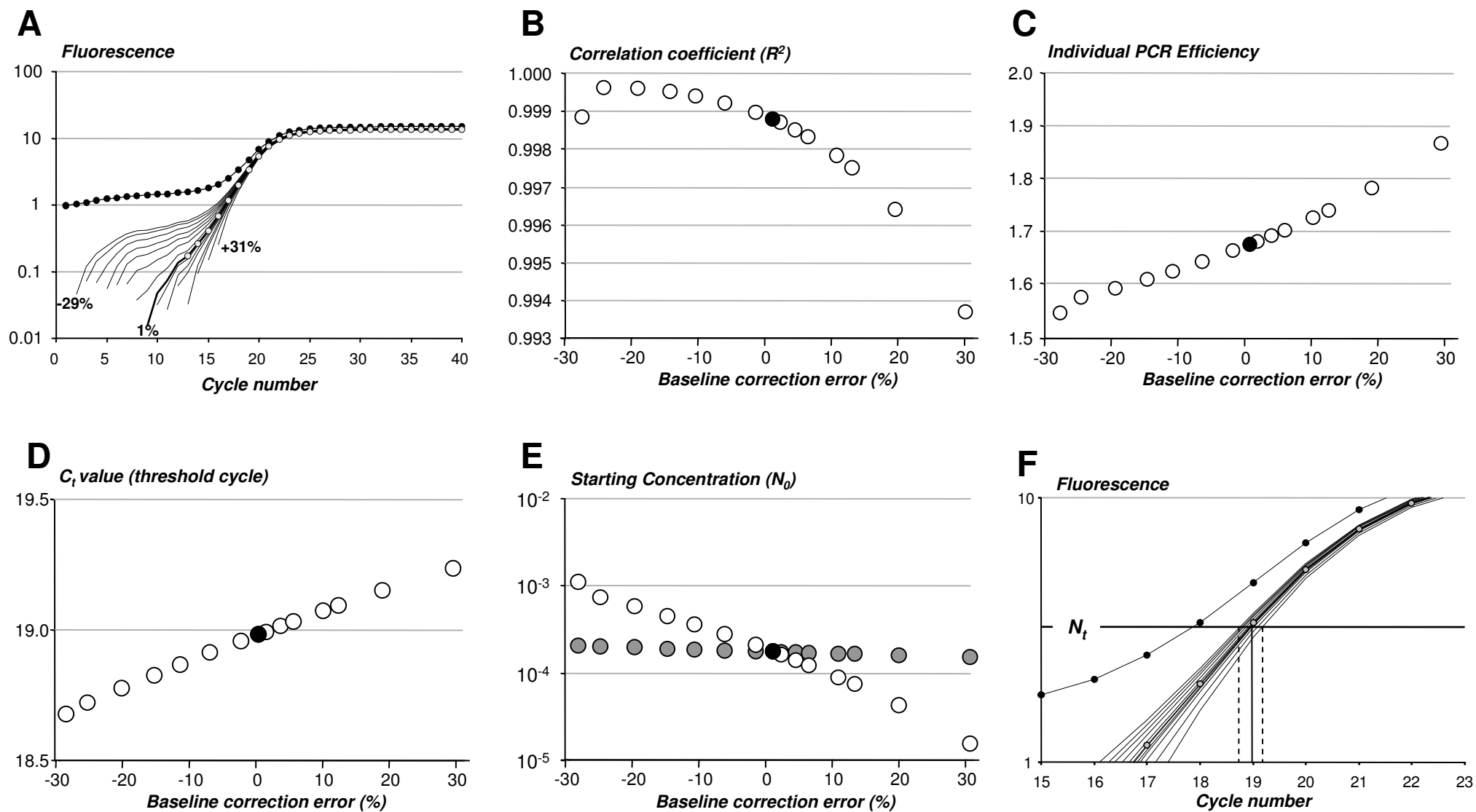
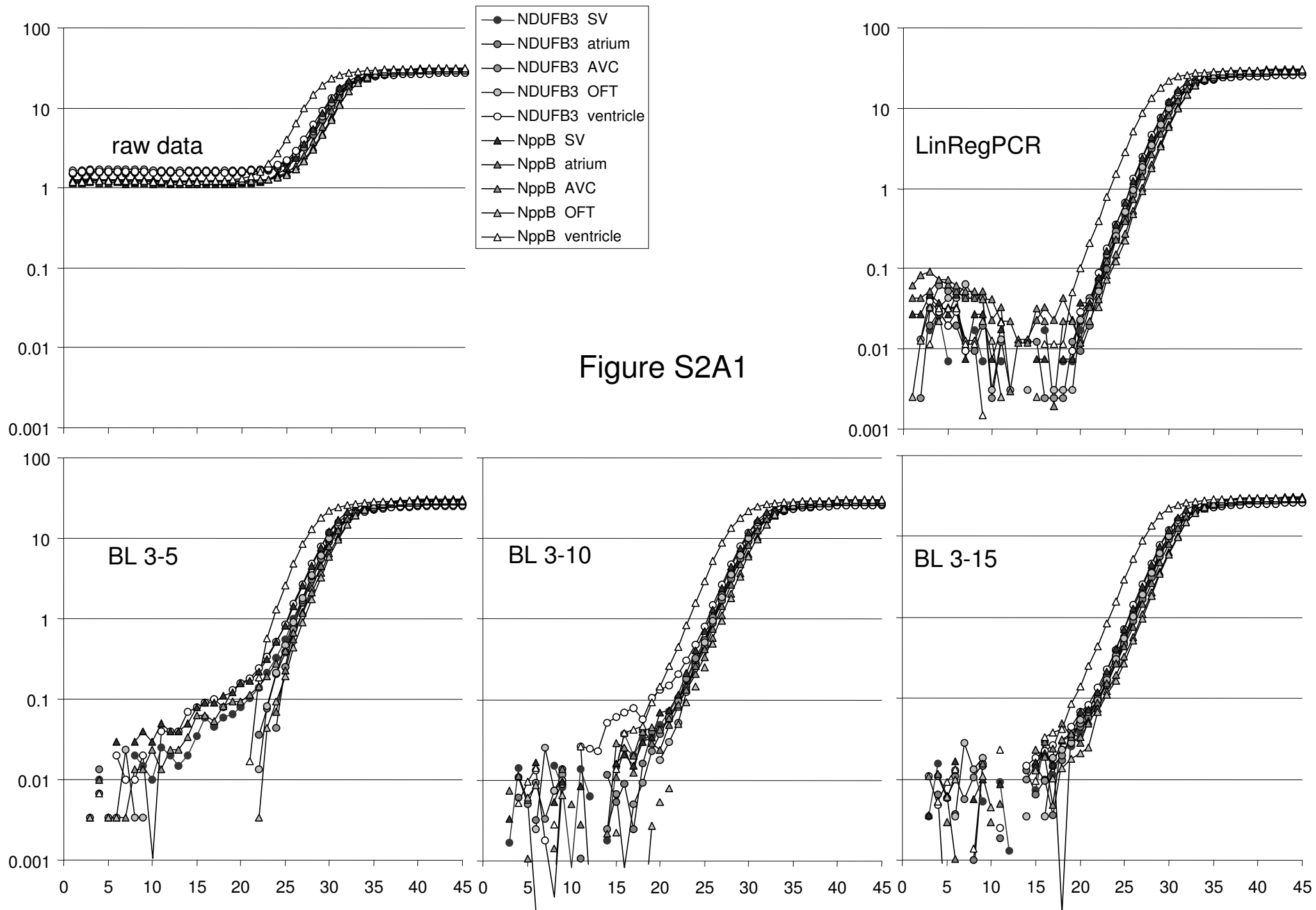
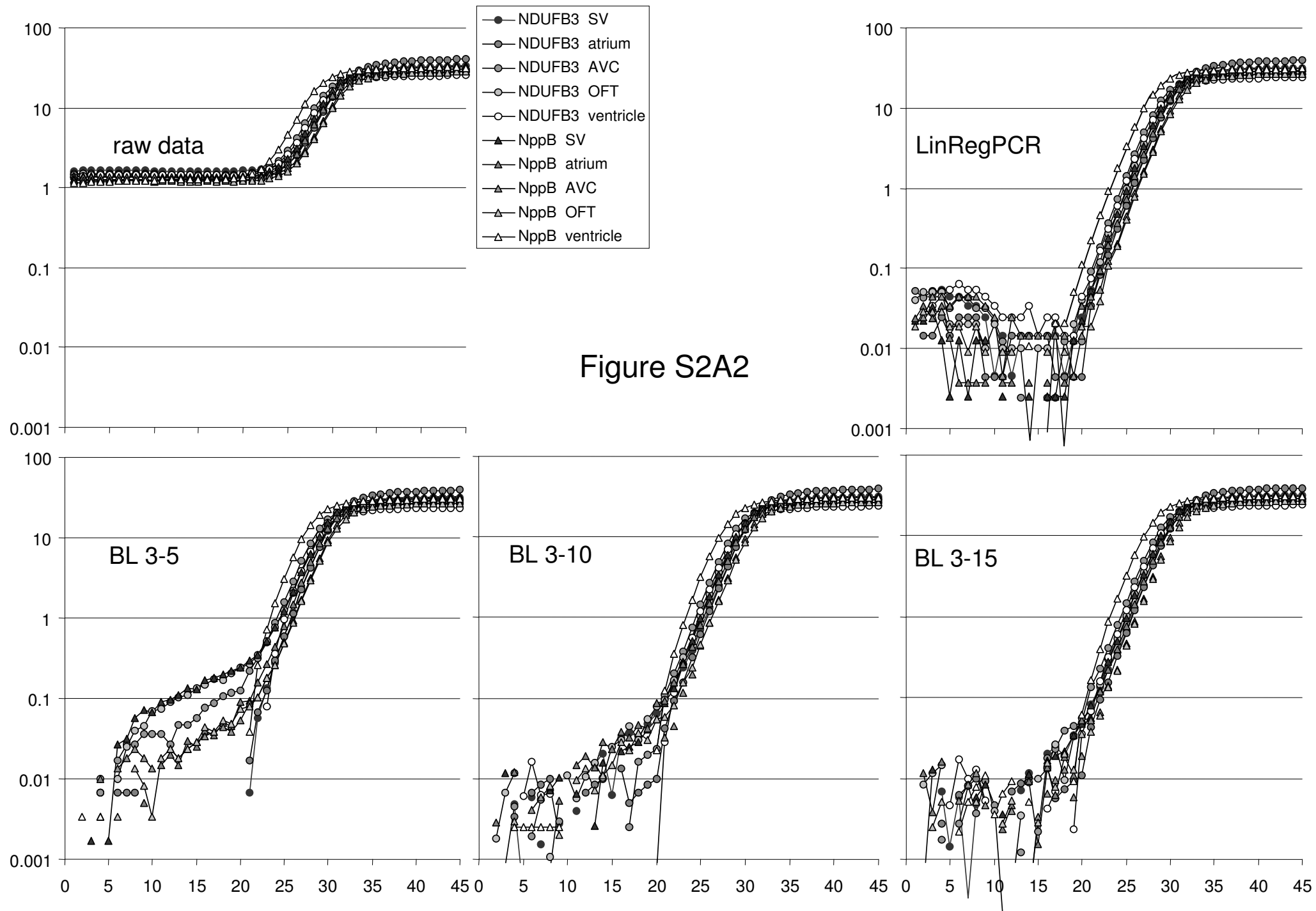
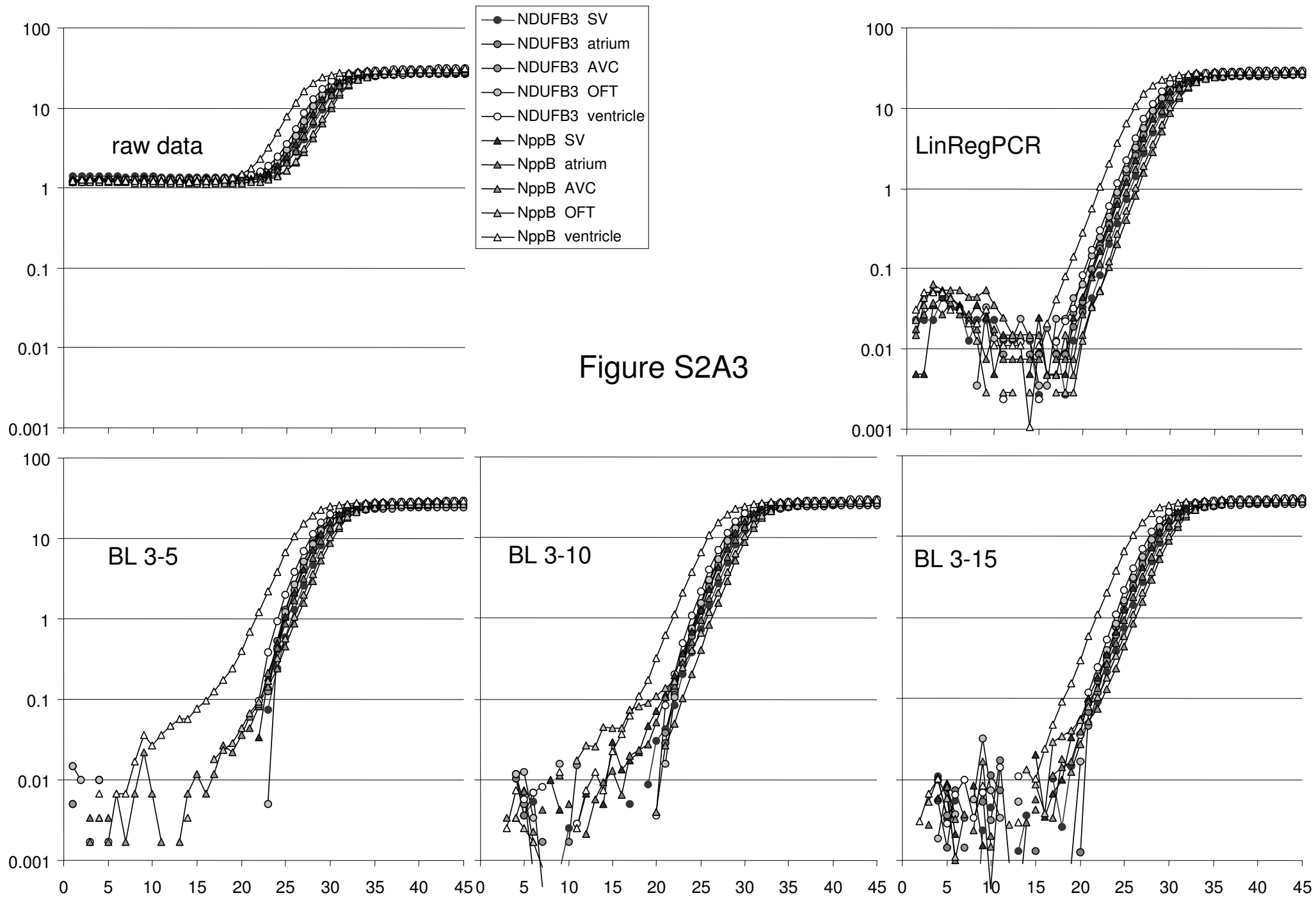


Figure S1







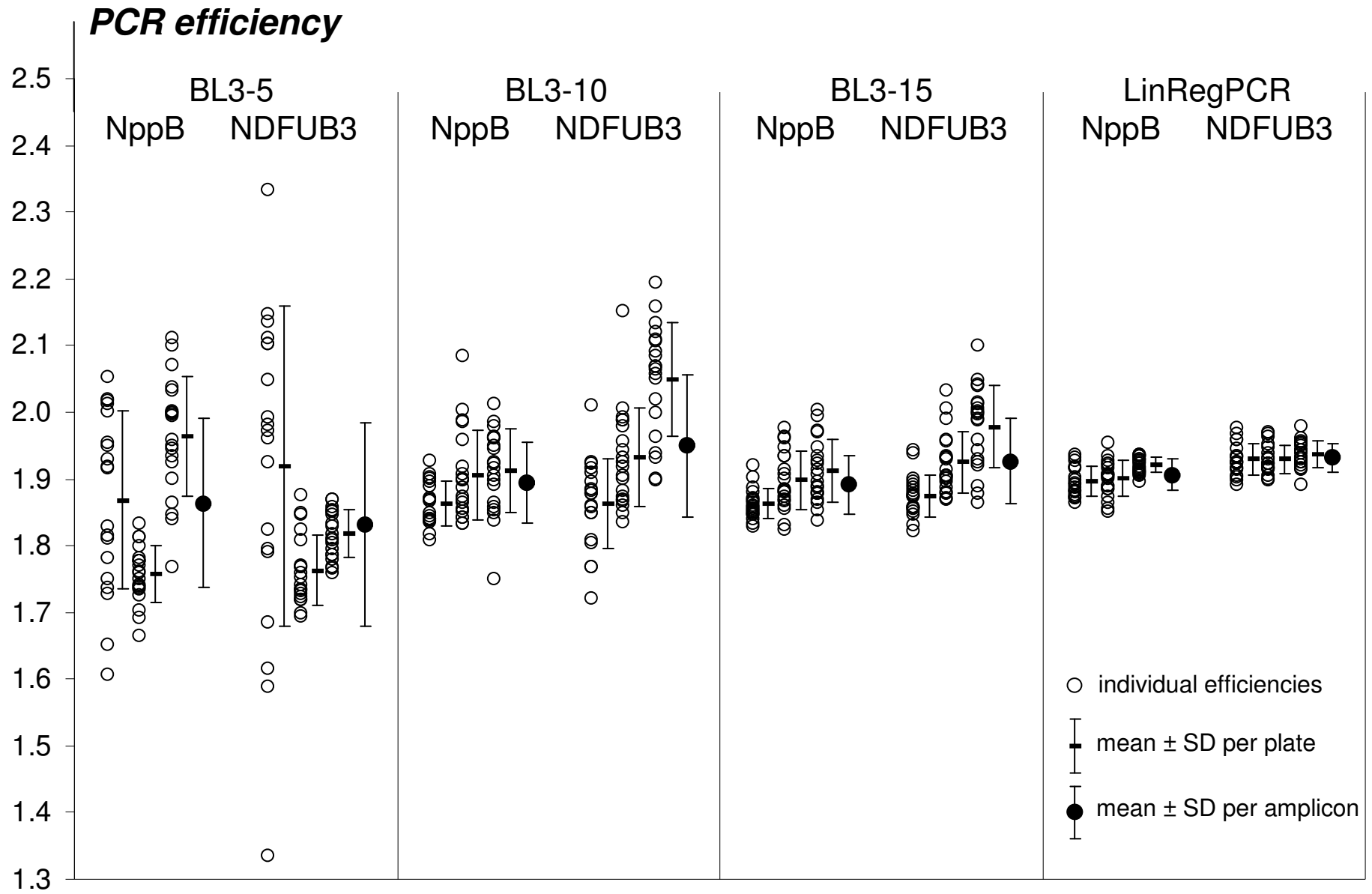


Figure S2B



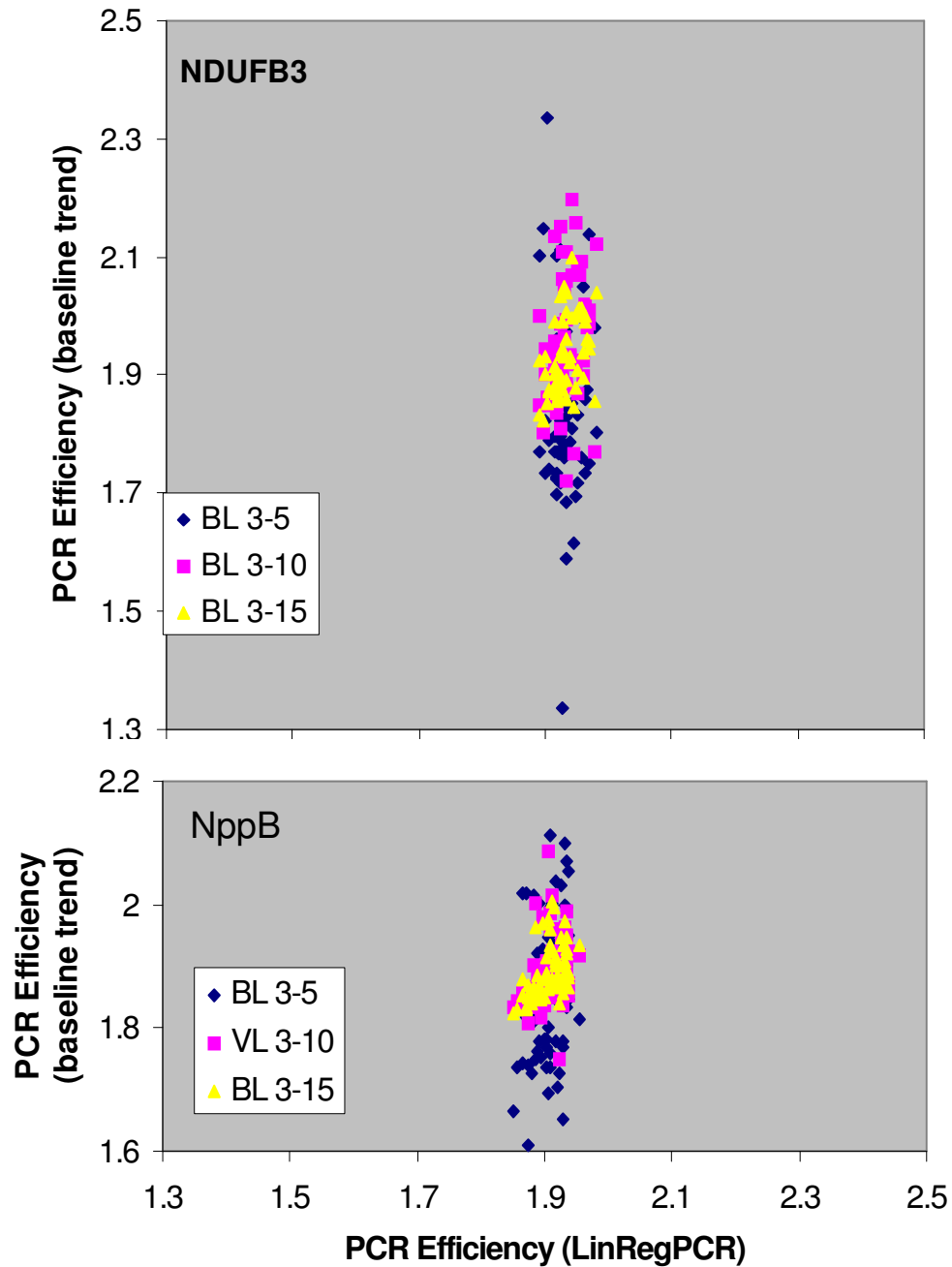
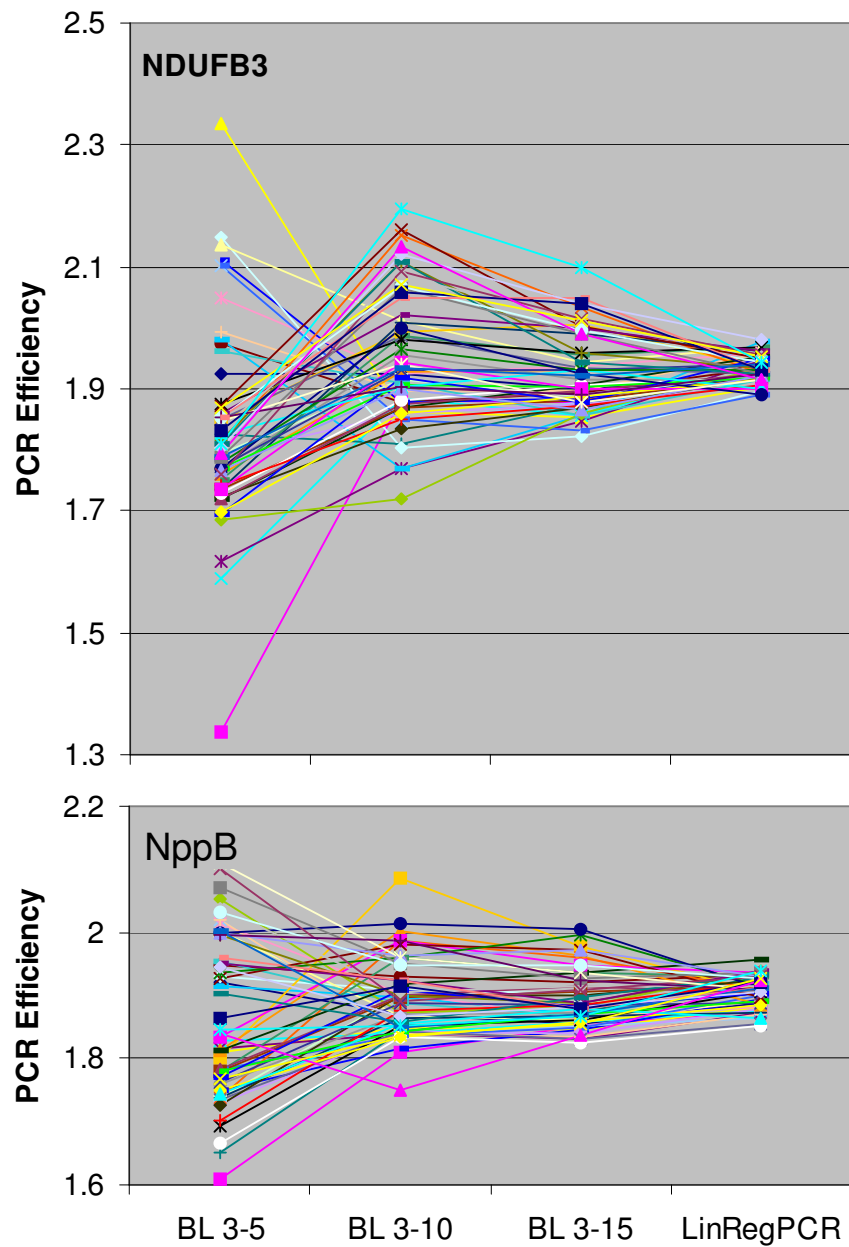


Figure S2C

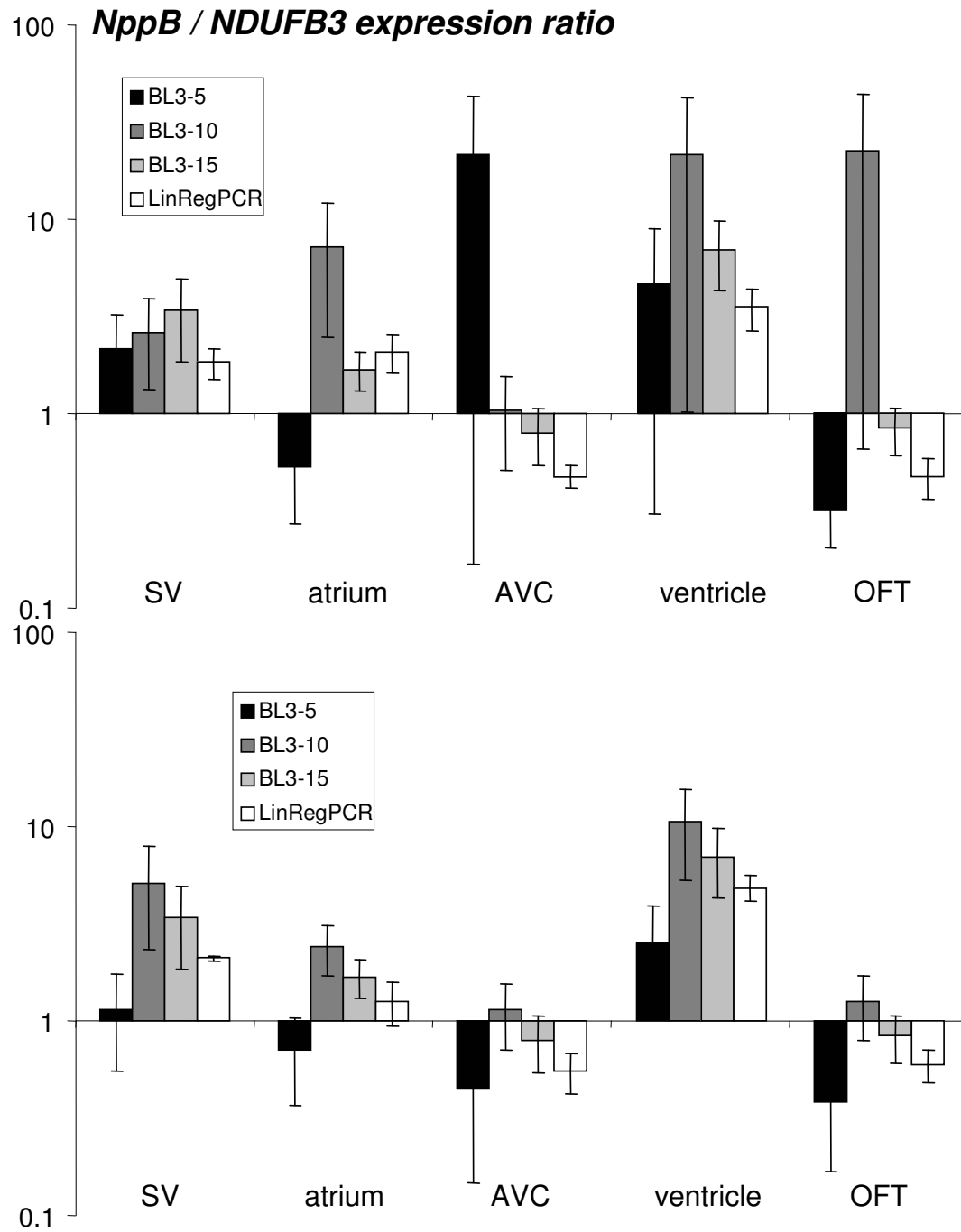


Figure S2D

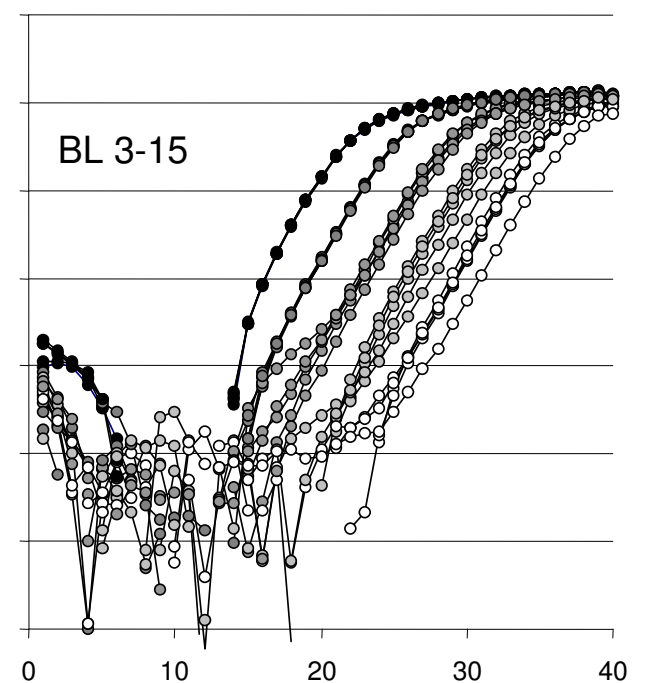
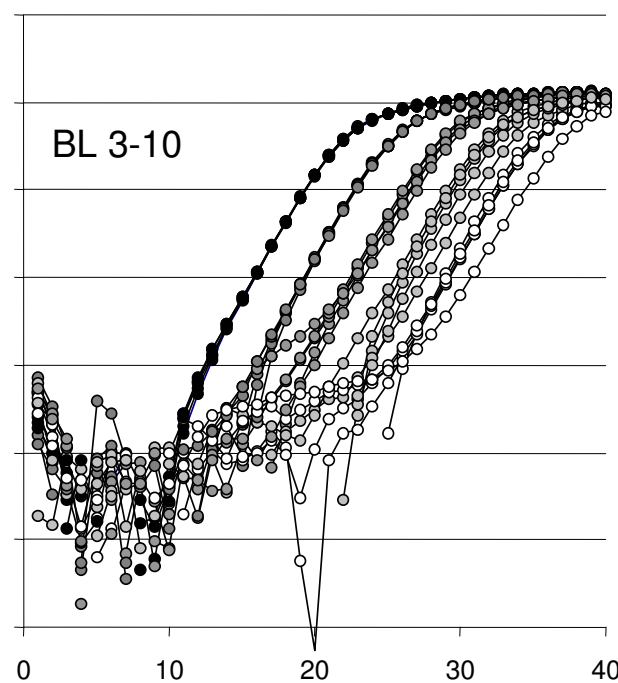
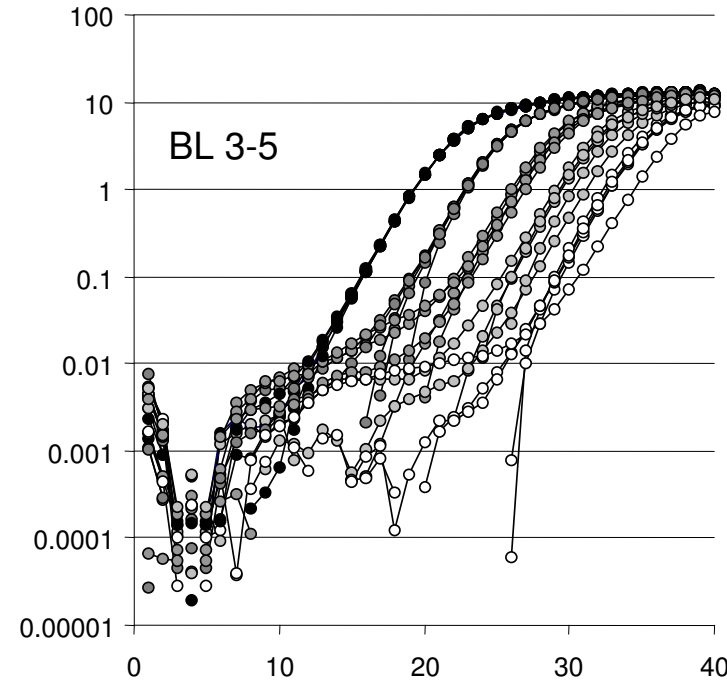
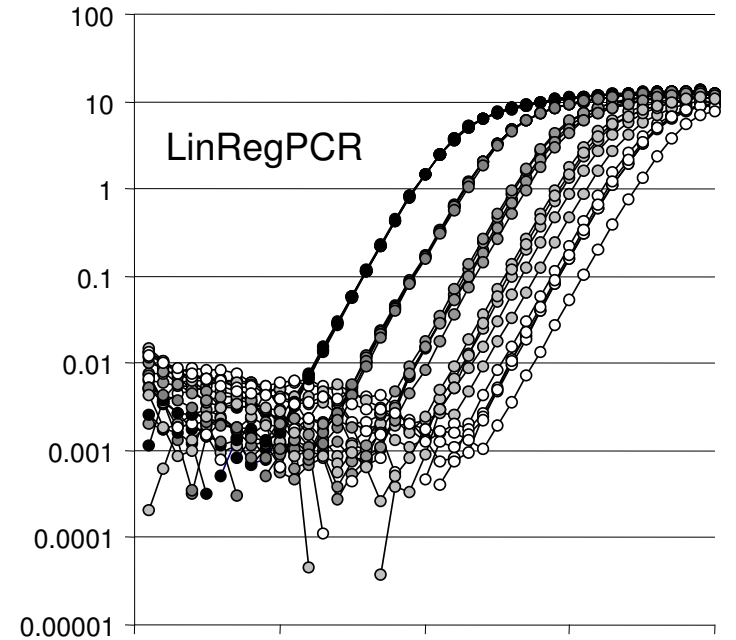
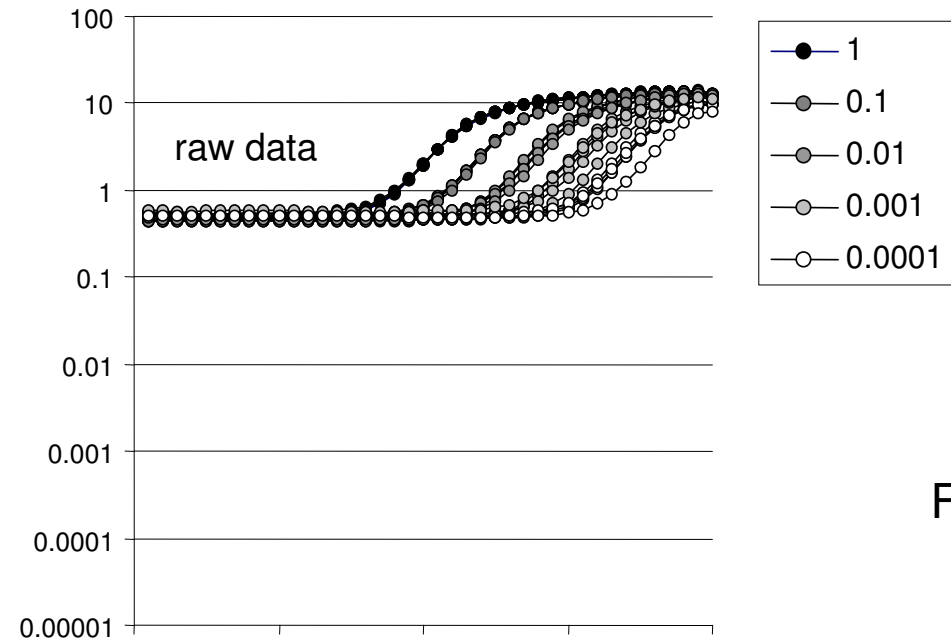


Figure S3A

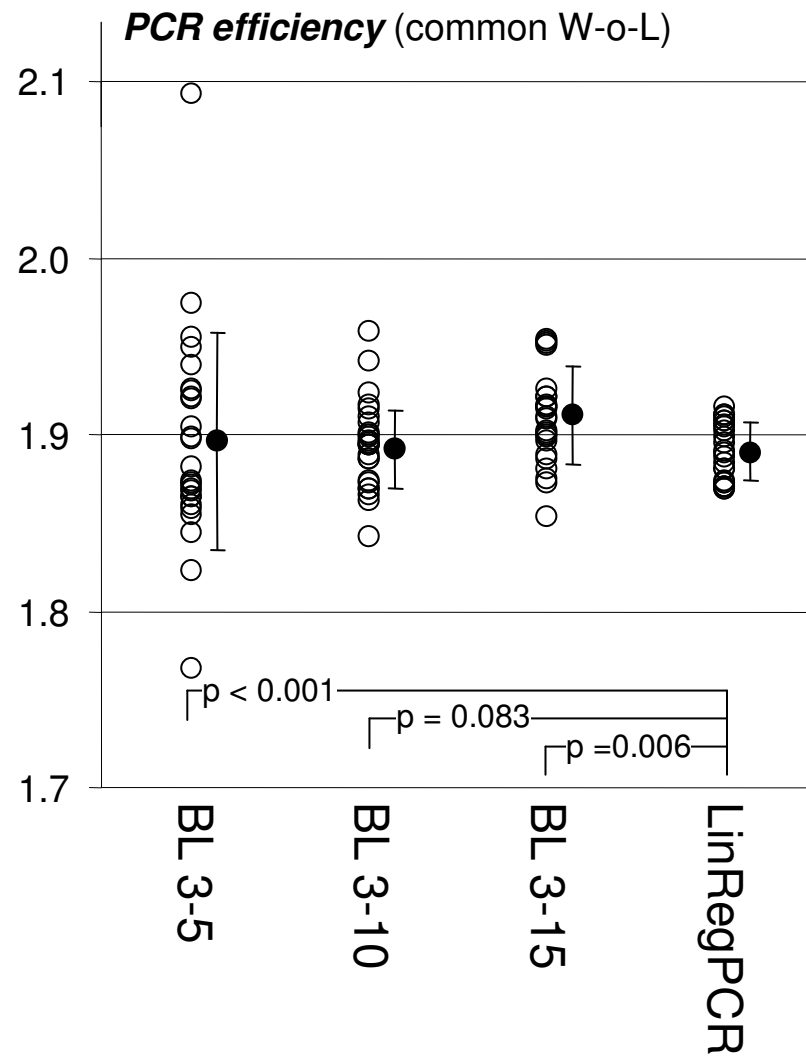
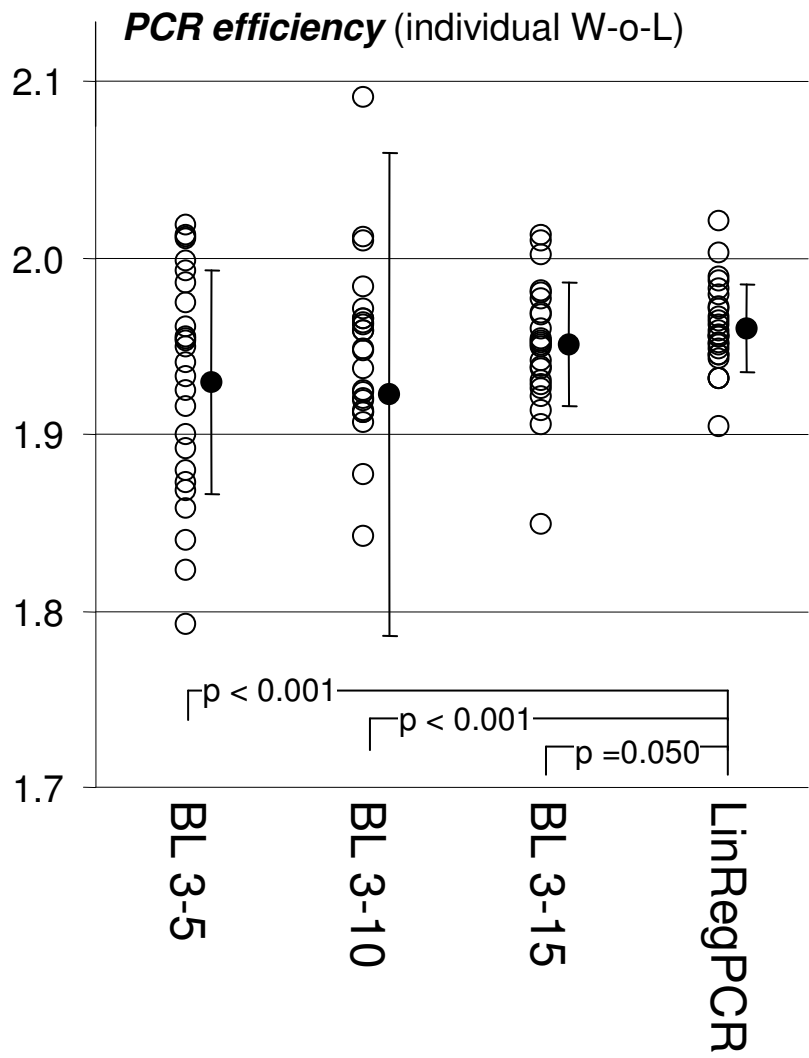


Figure S3B

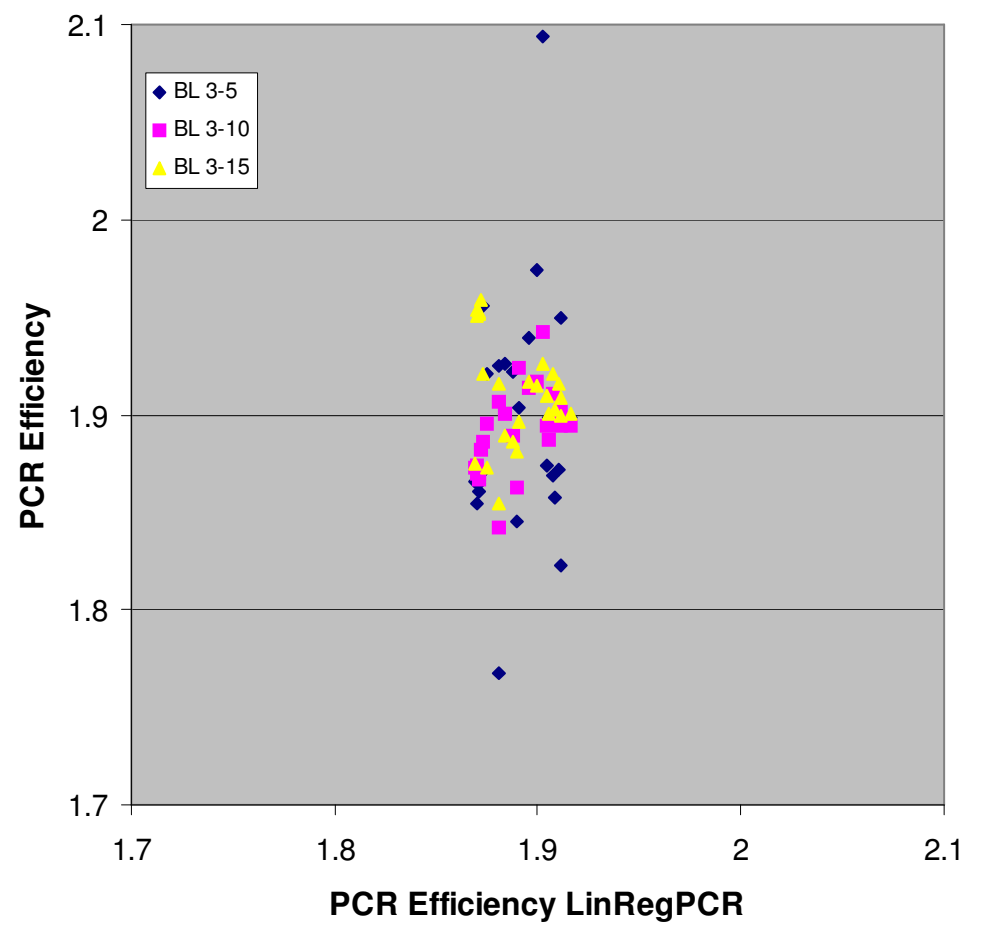
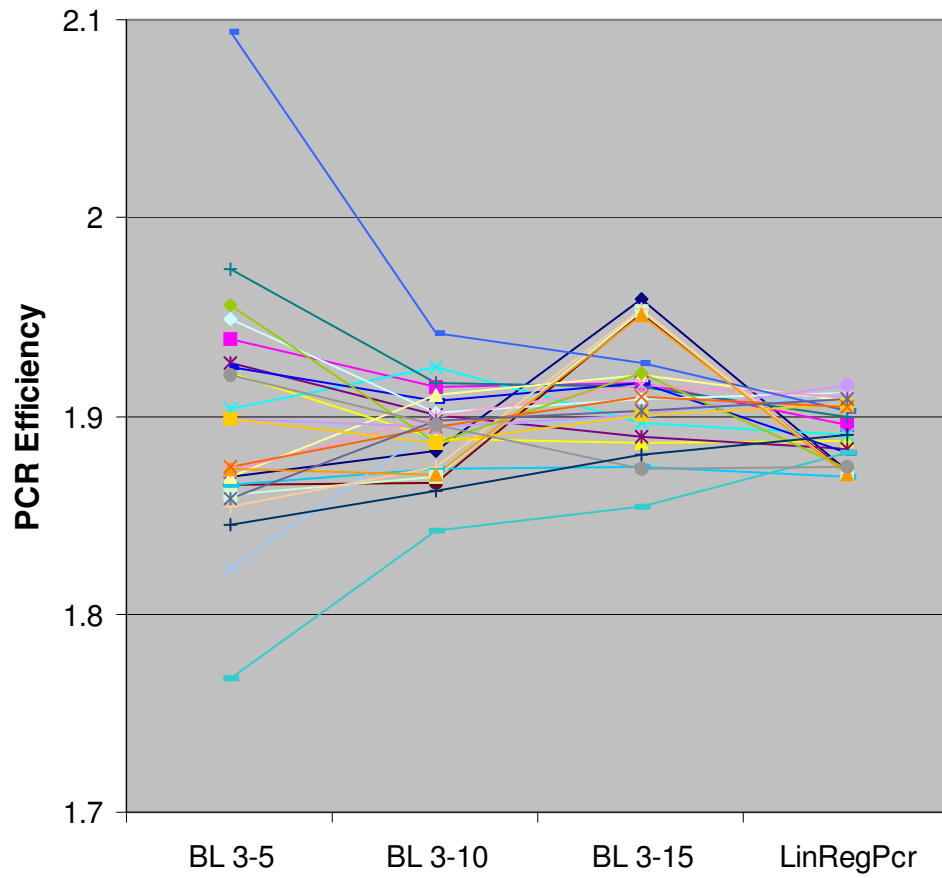


Figure S3C

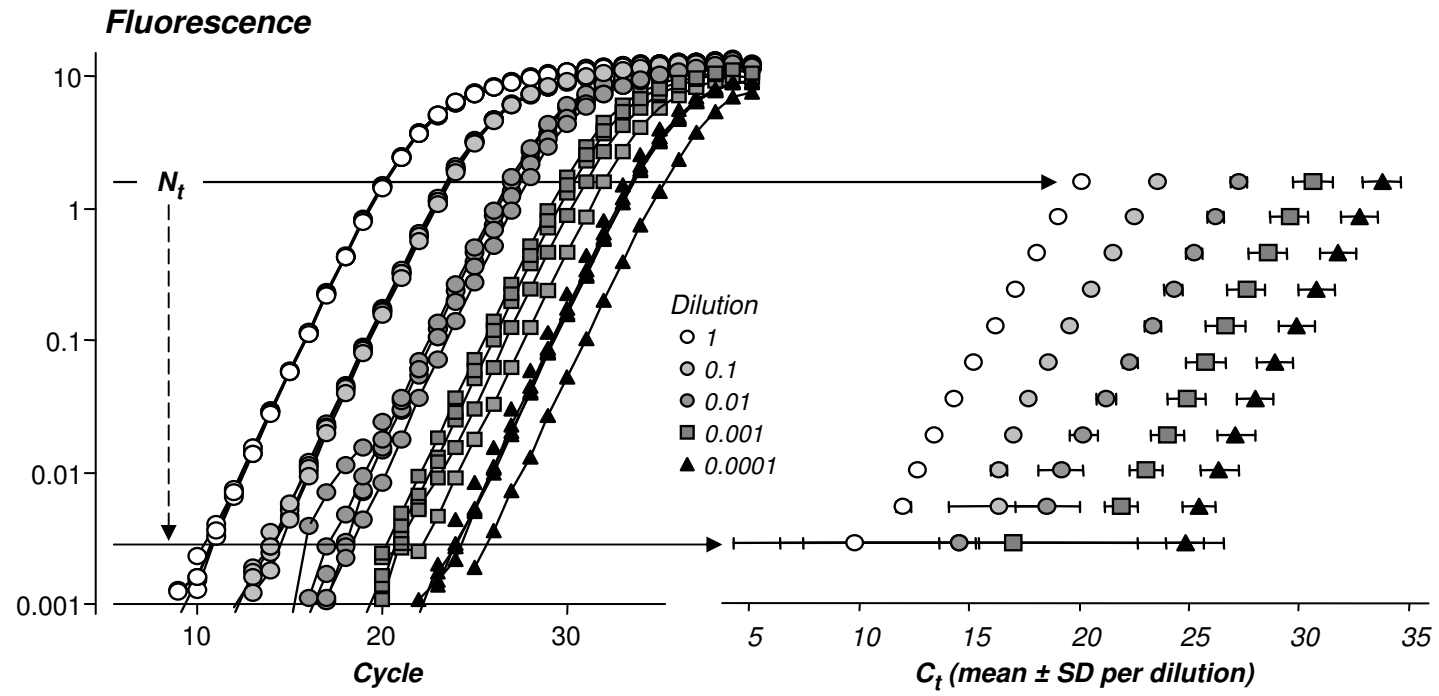


Figure S3D

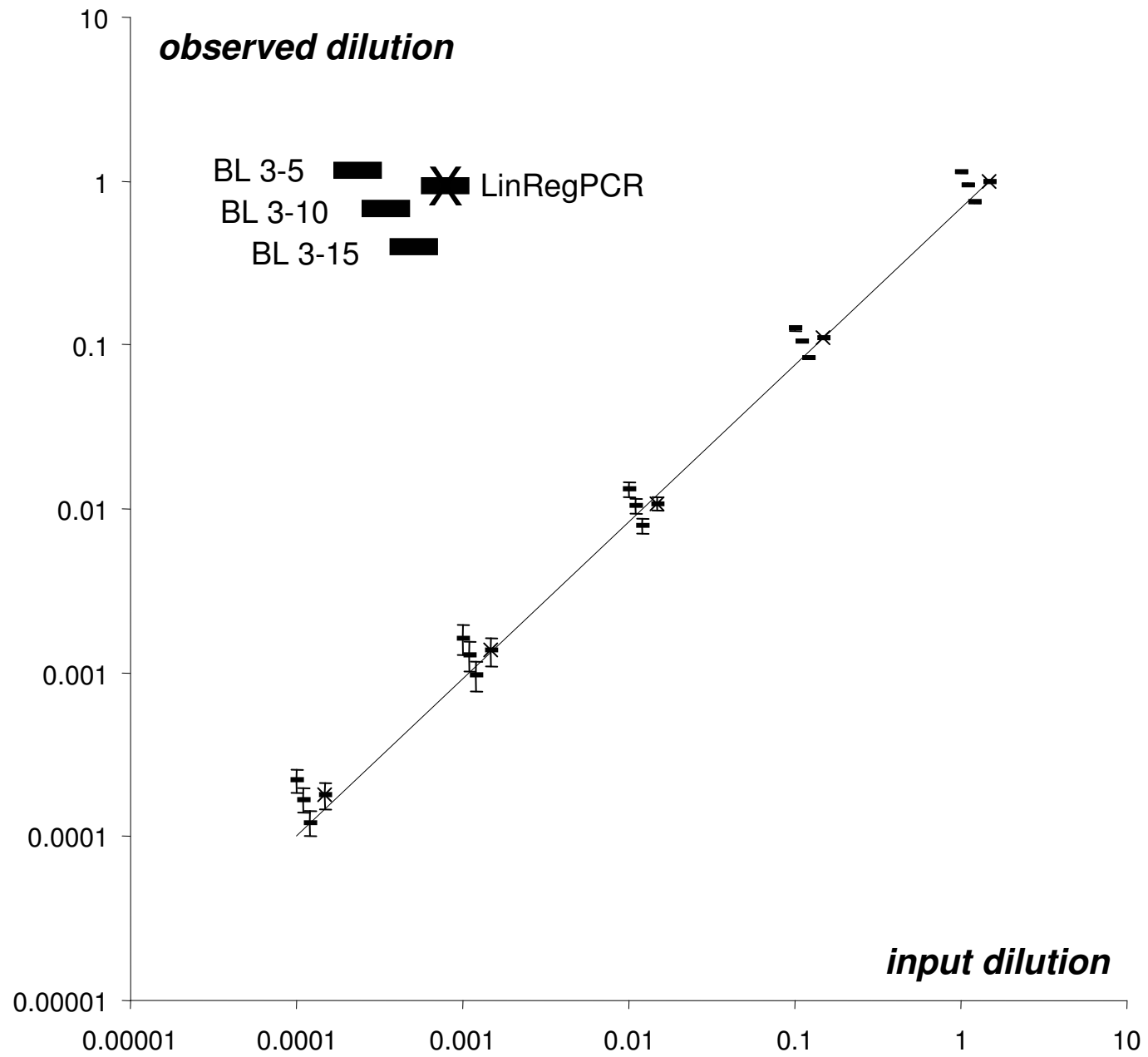
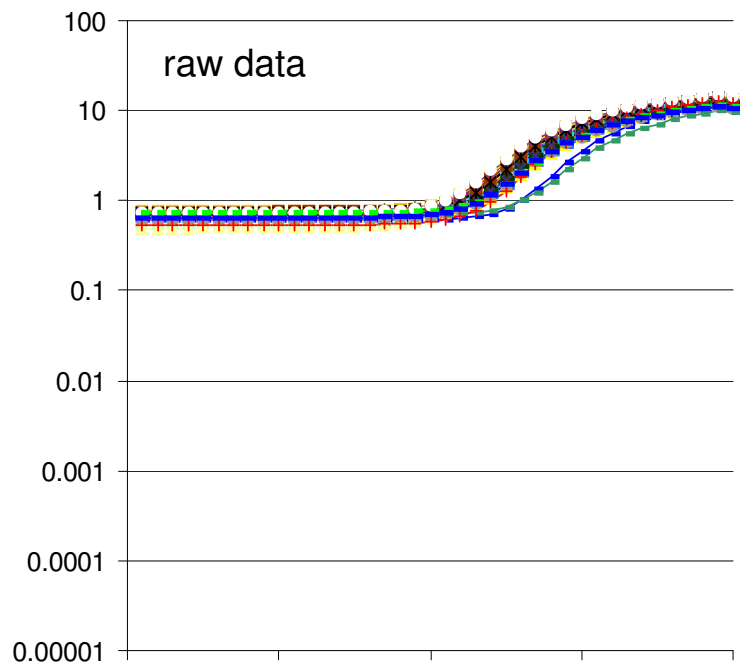


Figure S3E



PSMB5

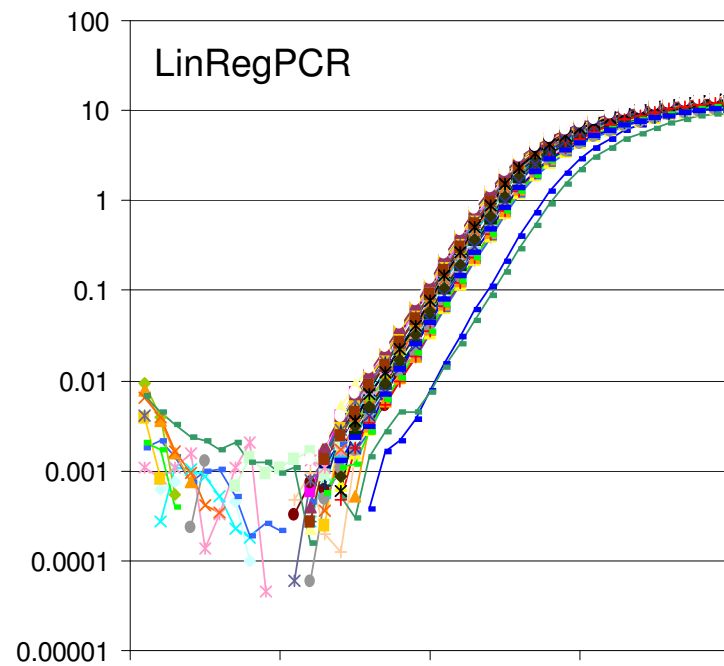
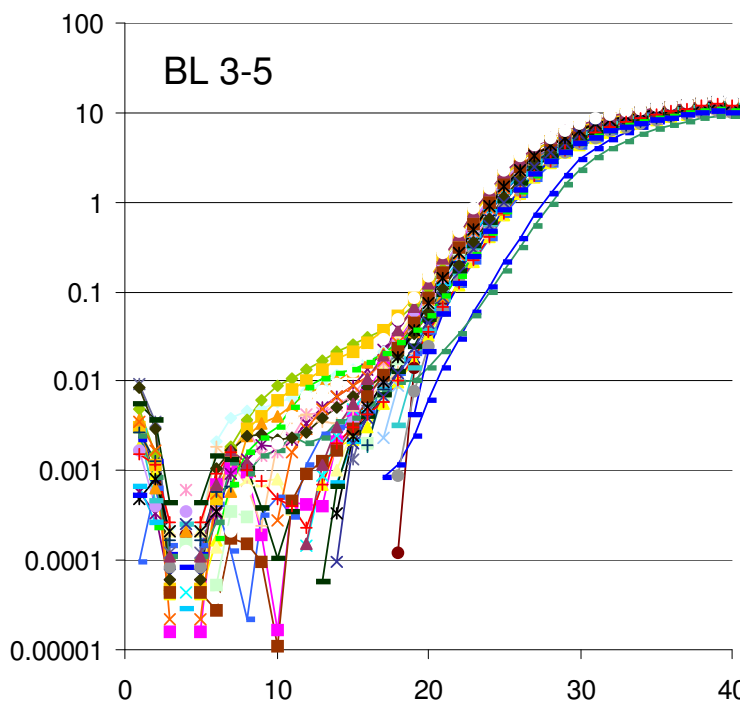
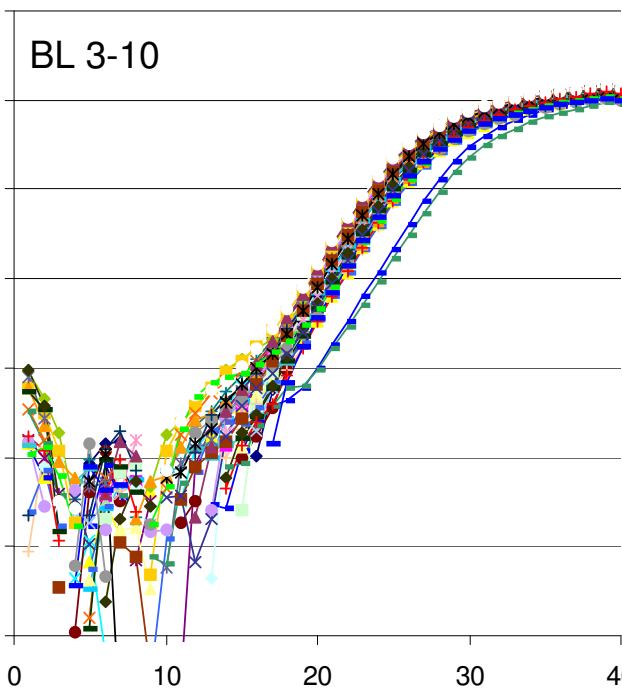


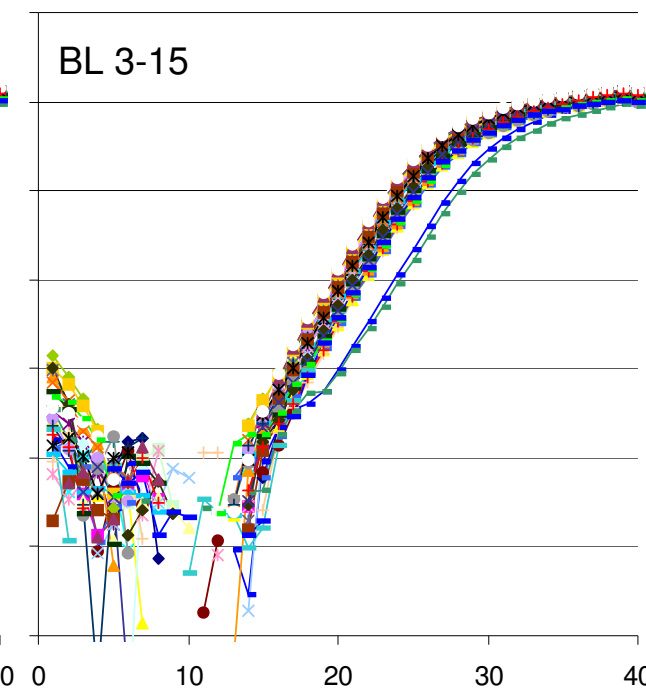
Figure S4A1



BL 3-10



BL 3-15





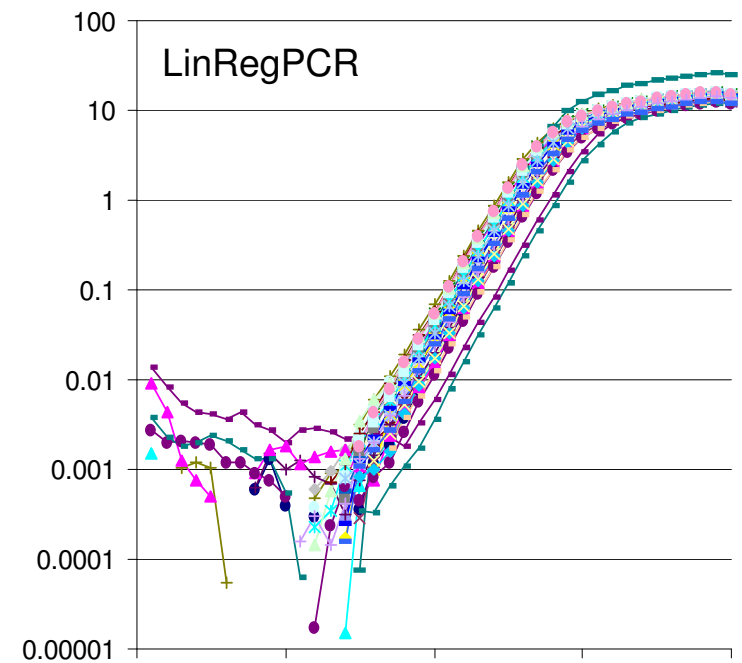
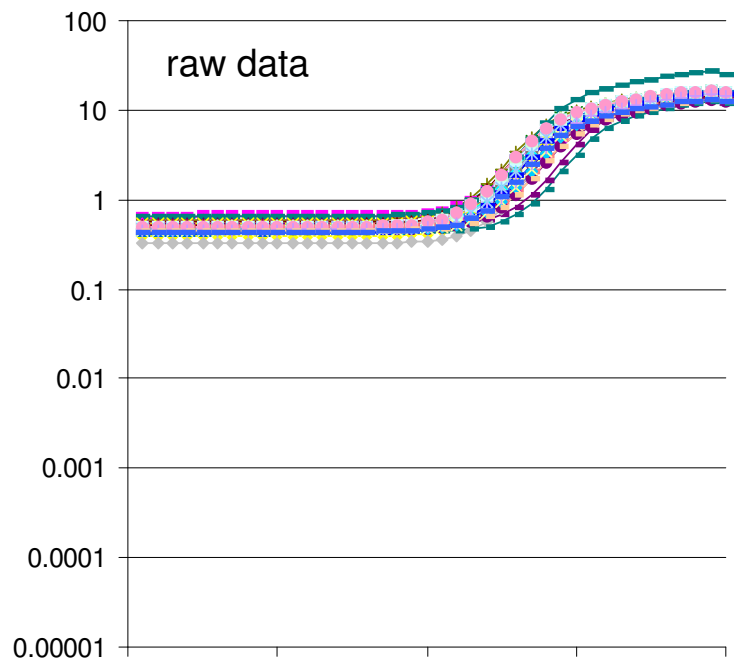
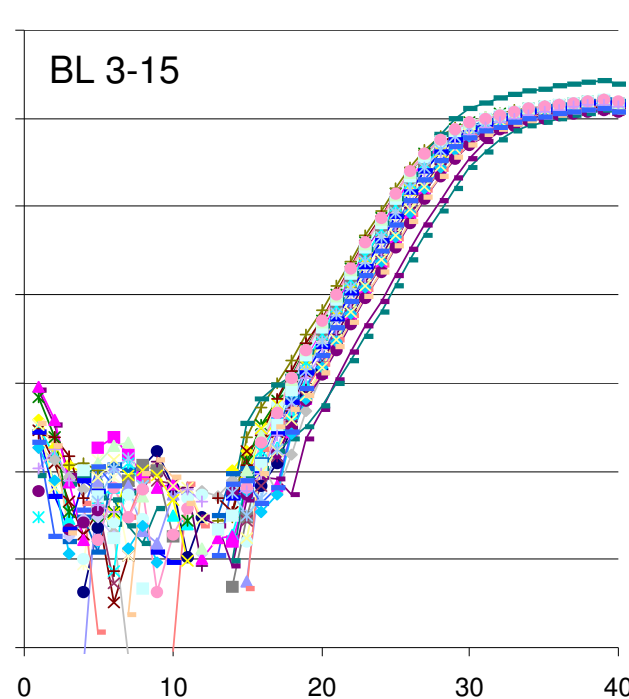
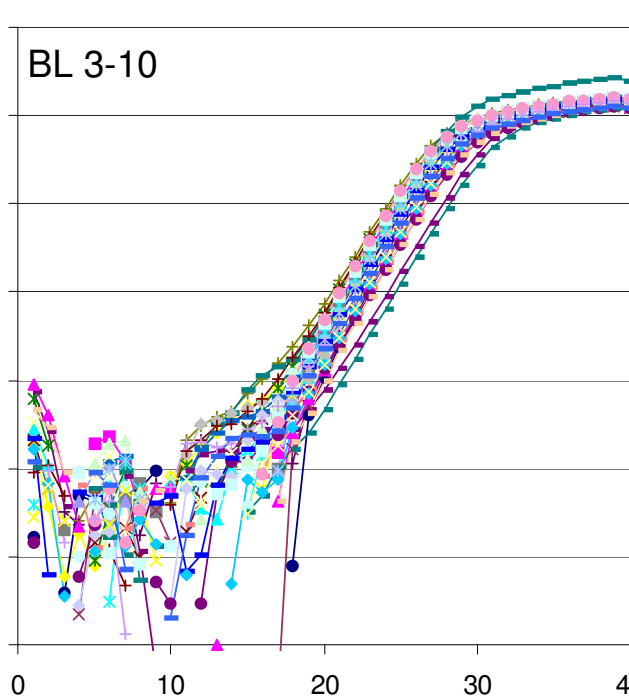
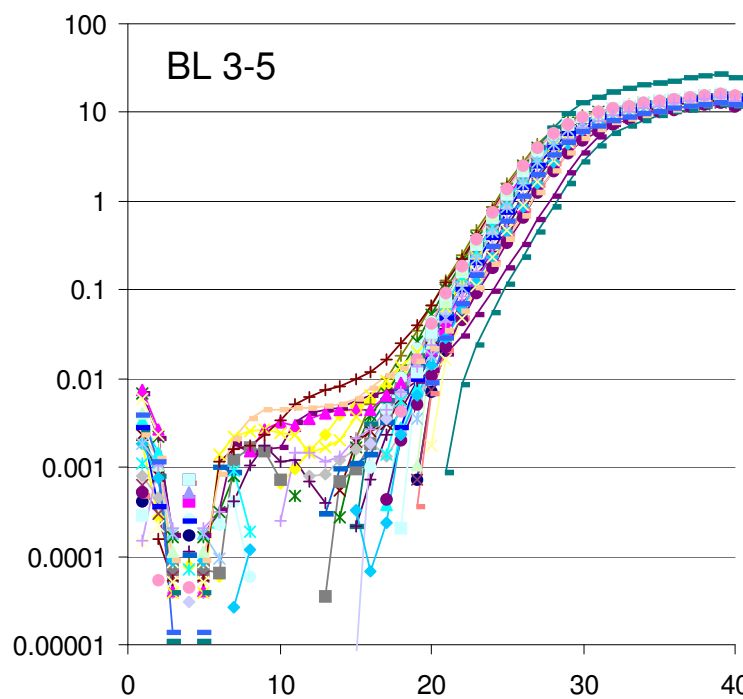


Figure S4A2



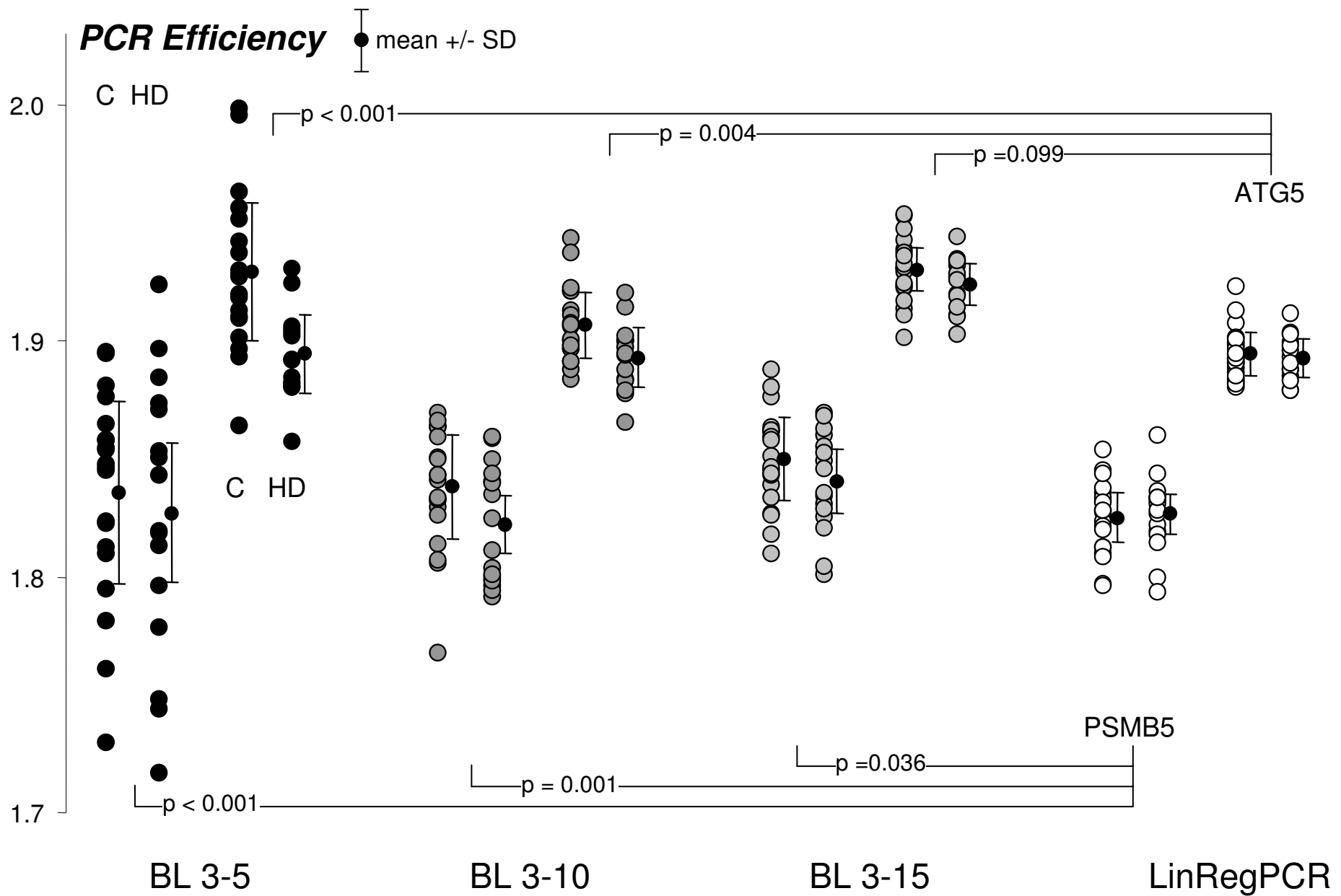


Figure S4B

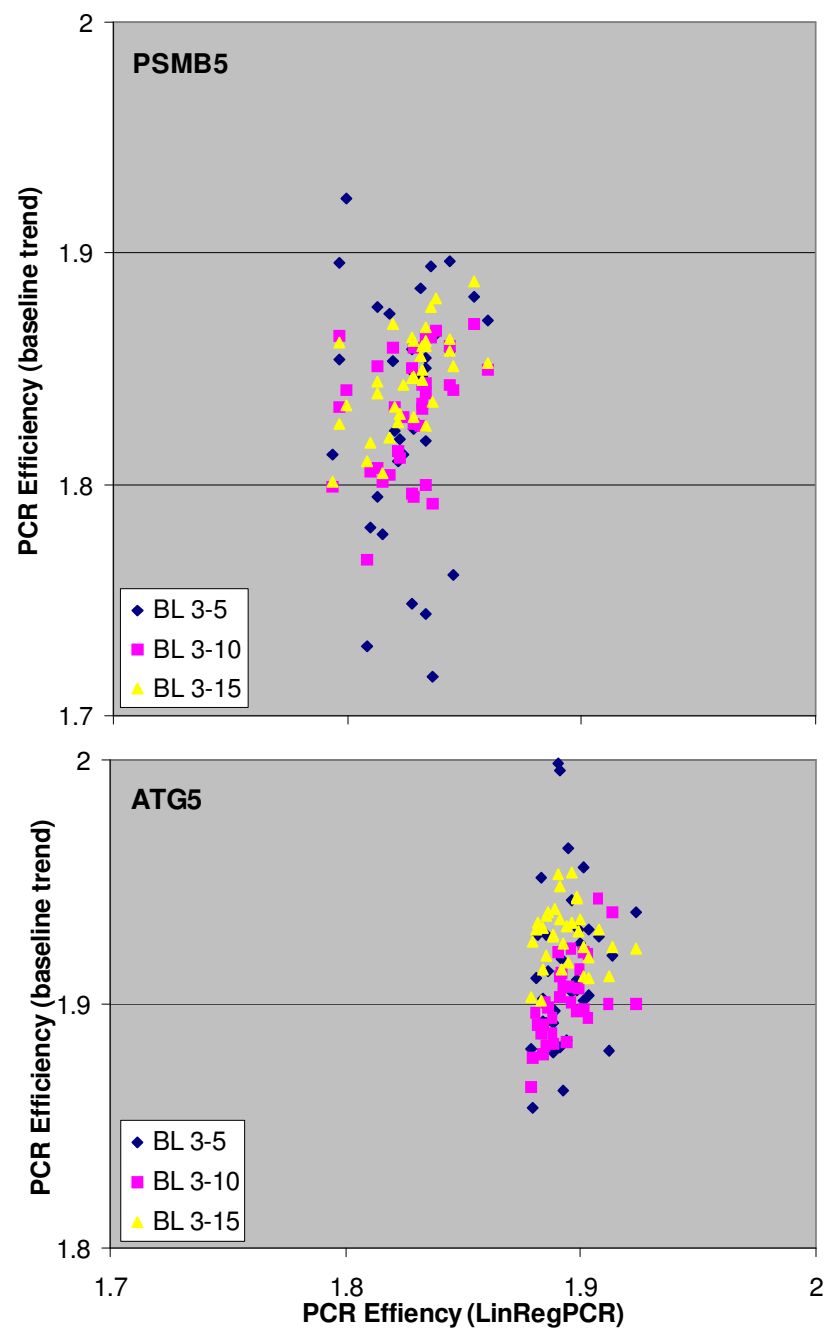
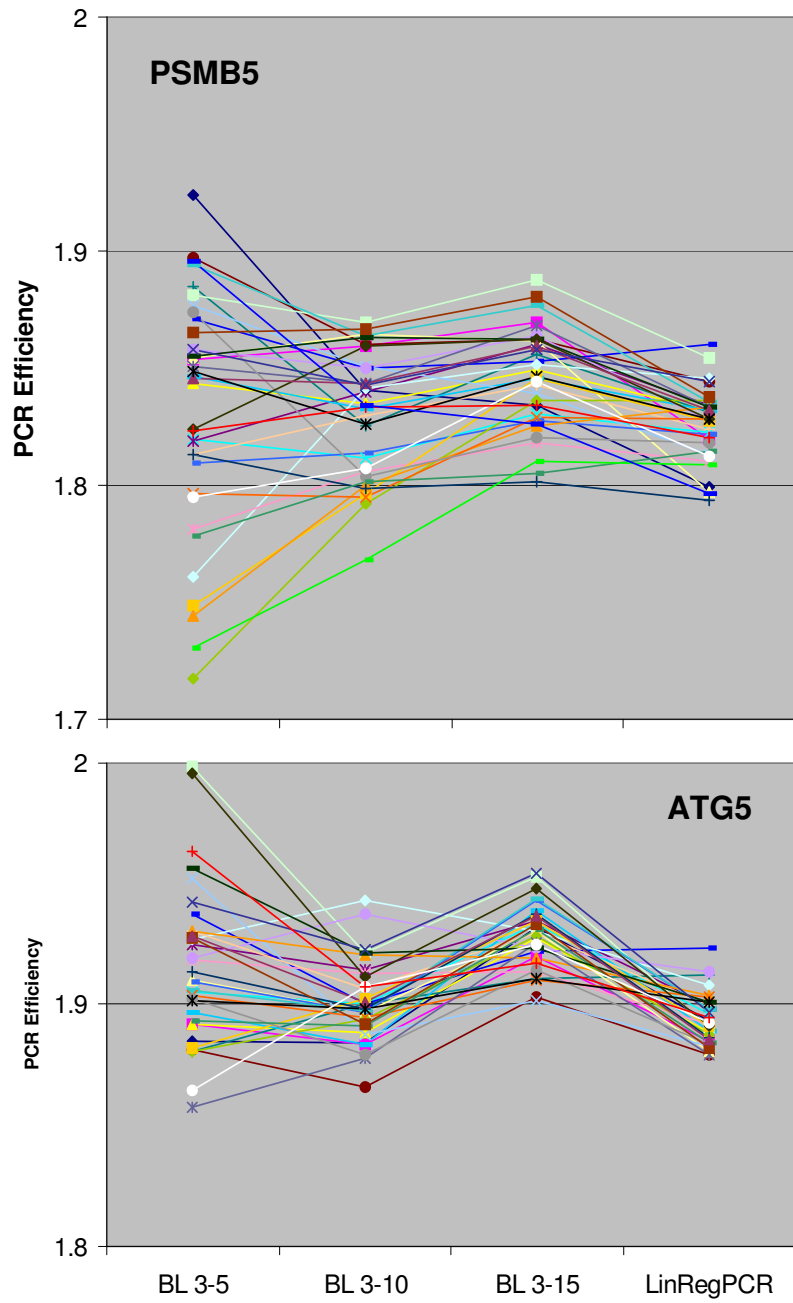


Figure S4C

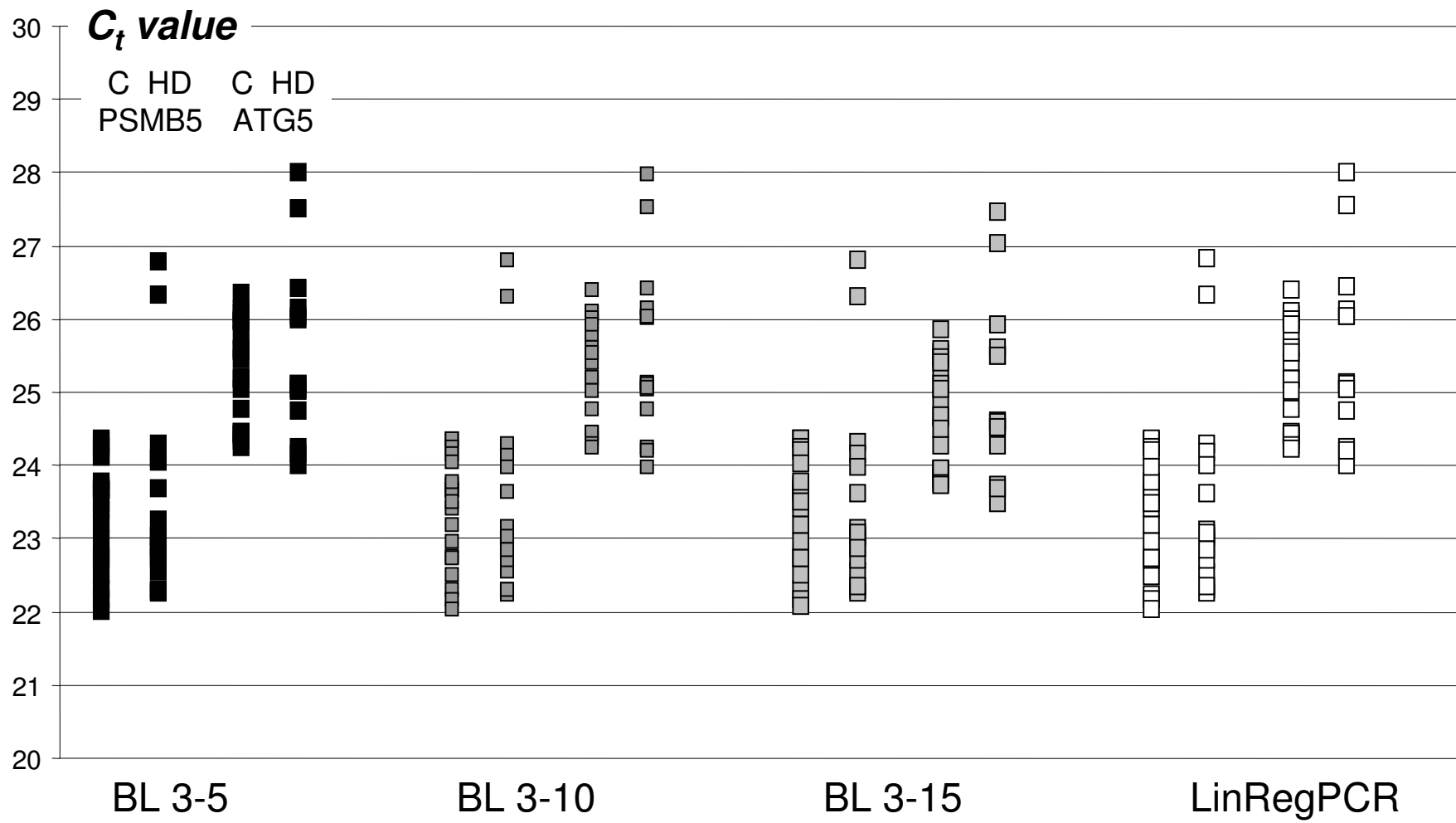


Figure S4D

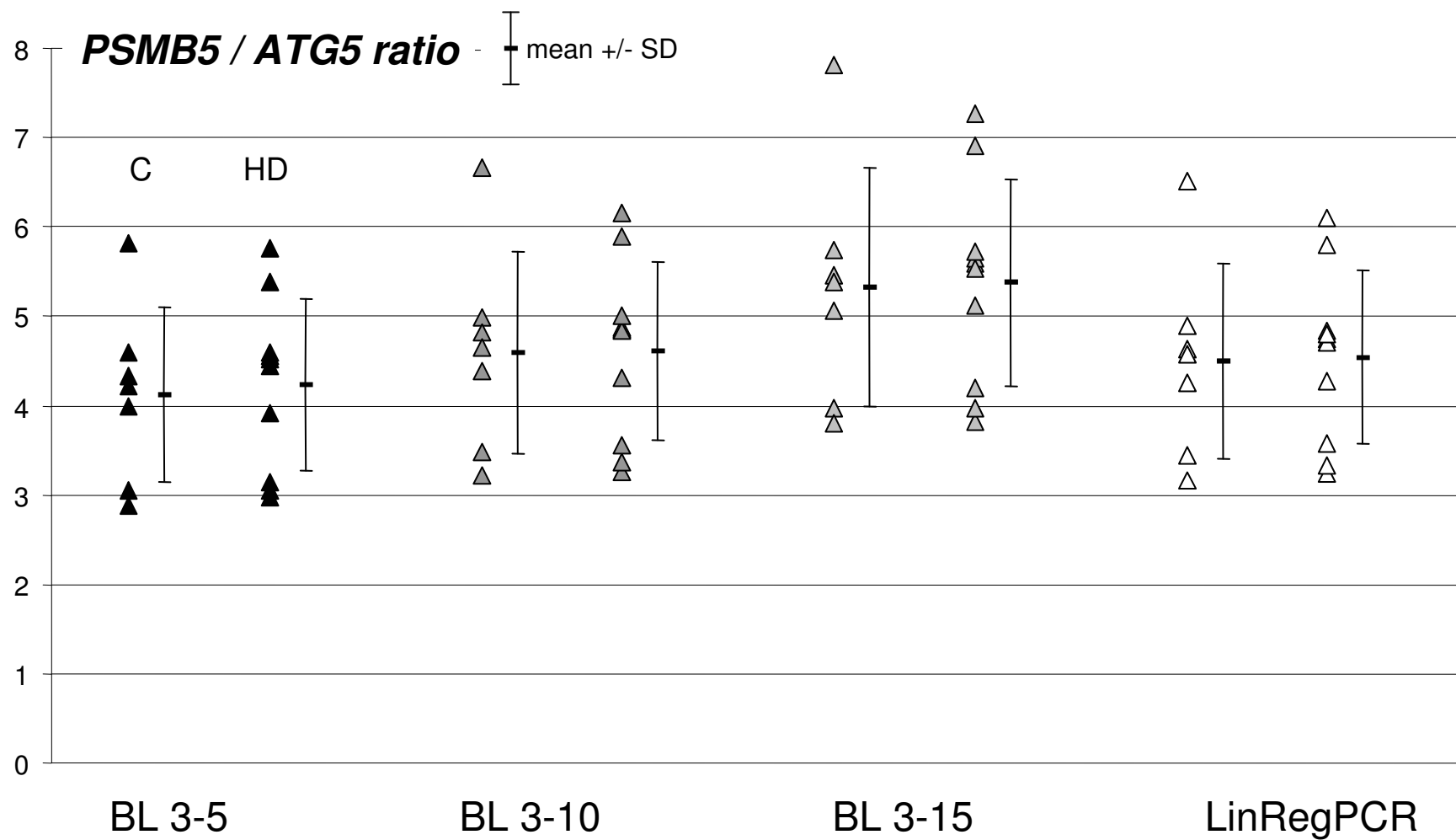


Figure S4E